

## EXPERIMENTAL INVESTIGATION OF THE CURRENT DENSITY AND THE HEAT-FLUX DENSITY IN THE CATHODE ARC SPOT

A. M. Esipchuk,<sup>a</sup> A. Marotta,<sup>a</sup> and  
L. I. Sharakhovskii<sup>b</sup>

UDC 621.387.143.014.31

*New experimental data on the effective "thermal" density of a current in the nonstationary arc spot on the copper cathode of an electric-arc heater of a gas and its dependence on the magnetic field have been obtained by thermophysical methods. Results of the investigation can be used for thermal calculations of electrodes for the purpose of increasing their service life.*

**Introduction.** In electric-arc heaters (EAHs), an arc discharge initiated between two electrodes – the cathode and the anode – is used for heating a gas to high temperatures. In different heaters, the electrodes can differ in both the material and the design. The current is transferred from the arc plasma to the body of the electrode through special bounded regions on its surface called arc spots. In these spots, heat fluxes having a very high density can arise, which progressively and inevitably break down the electrodes. Since the heat-flux density in the arc spot is directly related to the current density formed as a result of complex microprocesses in the near-electrode plasma, it was always of great interest to investigators who considered the current density as a key to understanding these processes. The highest density of the current and of the heat flux and, as a consequence, the highest level of erosion are characteristic of the so-called "cold" electrodes (especially of the cathode) made of metals with a relatively low fusion temperature (for example, copper).

The density of the heat fluxes in the arc spots on cold electrodes is very high. Because of this, to prevent an instantaneous breakdown of the electrodes, the arc is moved rapidly using a magnetic field or a vortex gas flow. The electrophysical and heat processes in such moving spots on a cold cathode are characterized by a complex and dynamic space-time structure. It manifests itself in the fact that in the cathode macropot, a great number of other smaller microspots exist simultaneously; these microspots are in a continuous chaotic process of coalescence into denser groups that then break down. It has been shown experimentally using high-speed electron-optical devices [1, 2] that as the current in the cathode and the cathode temperature increase, dense associations of microspots with overlapping temperature fields ("second-kind spots") become dominant on the cathode. When the current and the temperature decrease, they experience a reverse breakdown into individual disconnected microspots that practically do not interact ("first-kind spots").

The current density in such spots is very difficult to measure. Traditionally, it was determined through the measurement of the current in the arc spot and the area of this spot. However, it is very difficult to measure the true size of the current-conducting zone in such a complex dynamic formation as the nonstationary arc spot. For these purpose, two methods were usually used – the method of autographs, in which the size of the spot was identified with the erosion mark made by it on a special coating, and the method of high-speed optical recording, which made it possible to determine the size of the luminous region of the spot.

---

<sup>a</sup>Gleb Wataghin Institute of Physics, Campinas State University, Campinas, Brazil; email: aruy@ifi.unicamp.br; <sup>b</sup>Academic Scientific Complex "A. V. Luikov Heat and Mass Transfer Institute," National Academy of Sciences of Belarus, Minsk, Belarus; email: leonid@ptlab2.itmo.by. Translated from *Inzhenerno-Fizicheskii Zhurnal*, Vol. 74, No. 3, pp. 198–206, May–June, 2001. Original article submitted September 25, 2000.

TABLE 1. Current Density  $j$  ( $10^9 \text{ A}\cdot\text{m}^{-2}$ ) in the Arc Spot on a Copper Cathode for Different Currents (the data have been taken from [1] and obtained by different authors)

$I$	$j$
2.6	1.2
1–5	0.4–0.6
60	30–100
200	0.02–0.1
2–200	1.5–77
3000	0.25
5–4000	0.3–1.0
5000	12–1200
16000	8–800
20000	50

The drawback of both methods is that they give no way of determining the degree to which the erosion region or the size of the luminous region correspond to the size of the zone through which the current is transferred from the arc plasma to the electrode [1, 2]. The results of such measurements depend on many subjective factors, such as the exposure time, the velocity of movement of the spot, the physical properties of the surface, and others. Table 1 presents data on the current density on a copper cathode, which have been taken from [1] and obtained by different authors by the above-described methods. As is seen from this table, the measurement data on the current density in the cathode arc spot which are available at this moment vary from  $2\cdot 10^7$  to  $1.2\cdot 10^{12} \text{ A}\cdot\text{m}^{-2}$  only for copper, i.e., they differ by almost a factor of five! This reflects the weaknesses of the procedures used. It is practically impossible to use such data for calculating the heat regime of electrodes, in which the most important parameter is the heat-flux density in the arc spot, which in turn is a function of the current density.

The heat-flux density can be measured in principle by thermophysical methods, for example, by recording the initial moment of fusion of the electrode surface in the arc spot. Such procedures make it possible to obtain the effective values of the heat-flux density and accordingly the current density, averaged instrumentally over the spot area. They seem to be the most suitable for thermal calculations of electrodes. The advantage of these methods is the absence of the need for measuring the dimensions of the conductivity zone of the spot, which are very difficult to carry out in practice.

In the macroscopic model of erosion of cold electrodes [3], the notion of the thermal volt-equivalent of an arc spot  $U$  is widely used. It is determined as the ratio of the heat flux in the arc spot  $Q_0$  to the current intensity  $I$  or as the ratio of the corresponding densities:

$$U = Q_0/I = q_0/j . \tag{1}$$

Thus, having measured the effective density of the heat flux in the arc spot, from (1) we can obtain the effective density of the current in it if the thermal volt-equivalent  $U$  is known, and, conversely, the heat flux density can be calculated from the current density. The data on the values of  $U$  for a copper cathode are presented, for example, in [4, 5] where the dependence of  $U$  on the magnetic field has been revealed, which is very important for electric-arc heaters with magnetic displacement of the arc. Some preliminary data on measurement of the heat-flux density and the current density in the cathode arc spot by thermophysical methods are presented in [4, 6]. The aim of the present work is to further refine these data and especially the dependences of the current density on the magnetic field.

**Experimental Setup and Experimental Procedure.** Most of the experiments were carried out on the setup of the Gleb Wataghin Institute of Physics at the Campinas State University (Brazil) (hereinafter

referred to as GWIP). Here, we do not present the design and operation of this setup, because they are described in [5] in detail. For comparison purposes, we also used the data obtained on the setup of the A. V. Luikov Heat and Mass Transfer Institute, National Academy of Sciences of Belarus (hereinafter referred to as IHMT), which is similar to the above-mentioned setup in design, but has a higher power and larger dimensions. The main units of both setups were ring coaxial uncooled electrodes between which an electric arc was initiated. The arc was moved using an axial magnetic field induced by two solenoids. The setup was designed for short-term (1–2 sec) experiments carried out under nonstationary temperature conditions of heating of the electrodes. Moreover, in comparative analysis we used the values of the current density obtained in stationary experiments on investigating the electrode erosion. These experiments were carried out on a setup having the same configuration, except that water-cooled electrodes operating under stationary temperature conditions were used instead of uncooled electrodes. All the electrodes were made of commercial copper.

The outer ring electrode of a coaxial setup was used as the cathode (see [5]). On the GWIP setup, such a cathode had an inside diameter of 42 mm and an outside diameter of 52 mm. The width of the cathode was 2 mm in all the experiments. The anode was 36 mm in diameter; hence the interelectrode gap was 3 mm. The operating parameters of the setup were varied within the following limits: the arc current was varied from 191 to 434 A, the magnetic-field induction from 0.01 to 0.38 torr, and the axial velocity of the plasma-forming gas from 0.2 to 0.9 m/sec. Compressed air without previous cleaning was used as the plasma-forming gas. For these characteristics, the velocity of the arc spot lay within the range 76–407 m/sec, and the mean-integral density of the heat flux entering the cathode was  $(0.5\text{--}1.8)\cdot 10^7$  W/m<sup>2</sup>.

The basic parameters of the experiment (electrode temperature, current in the arc, voltage across the arc, magnetic induction, gas flow rate, and others) were recorded on the hard drive of a computer. For control of the experiment, and acquisition and preliminary processing of data, a program was developed with the use of the LabView program shell. The hardware used in the experiment consisted of an AT-MIO-16E-10 plate and an SCXI-1000 Chassis communication interface (Signal Conditioning Extension for Instrumentation). This system shut off the setup automatically by a signal from a thermocouple that was mounted on the cathode upon attainment of a certain preassigned temperature.

The employed nonstationary method of measuring the heat flux is a modification of the known method widely used for thermal diagnostics of plasma and hypersonic flows with a high stagnation temperature (see, for example, [7]). The only difference was that instead of a plate, we used a calorimeter in the form of a short hollow cylinder (ring) whose function was performed by the electrode itself. Since the experiment was carried out within a short time interval and the losses of heat passed through the outer and the side surfaces of the ring in this period were negligibly small, its surfaces may be considered as heat-insulated, except for the inner surface in contact with the electric arc. The temperature field of such a calorimeter was calculated from the known solution of the problem of heating of an infinitely long hollow cylinder with a heat-insulated outer surface with boundary conditions of the second kind (i.e., for a constant heat flux  $q = \text{const}$ ) on the inner surface. A detailed description of the procedure used is given in [4, 5]; therefore, we do not present it here. We only note that the dimensions of the rings were chosen such that in the experiments we could obtain a regular regime of heat conduction in which the ring temperature changed linearly with time in accordance with the expression (see [4, 5])

$$q = \frac{\lambda}{a} \frac{R_2^2 - R_1^2}{2R_1} \frac{dT}{d\tau} = K \frac{dT}{d\tau}. \quad (2)$$

This expression allows one to calculate the heat-flux density  $q$  averaged over the inner surface of the ring from the rate of its heating  $dT/d\tau$  recorded in the experiments. Since for copper the ratio  $\lambda/a$  changes only slightly with temperature, the value of the derivative  $dT/d\tau$  is constant for a constant value of  $q$  and the

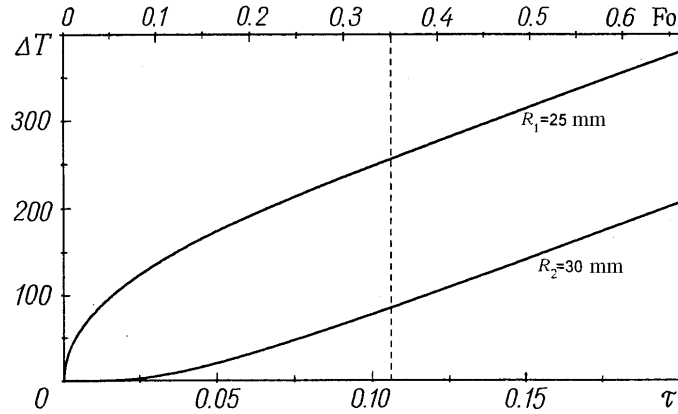


Fig. 1. Theoretical curves of heating of a copper ring calorimeter for its inner and outer radii ( $q = 2.7 \text{ kW/cm}^2$ ).

record  $T = f(\tau)$  (must be linear in character. As an illustration, Fig. 1 shows the theoretical curves of heating of a ring with an outer radius of 30 mm and an inner radius of 25 mm, which corresponds to the dimensions of the electrodes used in the IHMT setup. For plane calorimeters used in hypersonic aerodynamic setups, the point corresponding to the value of the Fourier criterion  $Fo = a\tau/\delta^2 = 0.35$ , where  $\delta$  is the thickness of the plate, is usually taken for the initial point of the linear portion of the function  $T = f(\tau)$  (see [7]). When the electrode begins to fuse, the linearity of the curve  $T = f(\tau)$  must break down and, simultaneously, the rate of temperature increase  $dT/d\tau$  must decrease because of the consumption of heat by fusion and the corresponding decrease in the heat flux to the electrode.

Hence, the mean-integral density of the heat flux entering the inner surface of the ring cathode can be calculated from the value of the derivative  $dT/d\tau$ , and the initial moment of fusion of the calorimeter surface can be determined from the moment when this derivative begins to decrease. As is seen from Fig. 1, the initial point of the linear portion of heating of the ring calorimeter corresponds approximately to the value

$Fo_{\delta} = a\tau \left( \frac{R_2^2 - R_1^2}{2R_1} \right)^2 = 0.35$ , as in the case of a plane calorimeter [7]. In the case of a ring calorimeter, in the expression for the Fourier criterion the effective thickness of the ring  $(R_2^2 - R_1^2)/2R_1$  is used instead of the plate thickness [8, 9].

The surface temperature of the electrodes was measured with the use of Chromel–Alumel thermocouples caulked in on the side surface of the cathode. It should be noted that to provide trouble-free operation of the thermocouples, they were positioned at a distance of 1.5–2.0 mm from the inner surface of the electrode. In this case, the surface temperature was calculated in terms of the temperature  $T(r)$  measured at the point with the coordinate  $r$  using the expression

$$T(R_1) = T(r) + \frac{q}{2\lambda} \frac{R_1}{R_2^2 - R_1^2} \left[ 2R_2^2 \ln \left( \frac{r}{R_1} \right) - r^2 + R_1^2 \right], \quad (3)$$

obtained from the general solution of the problem of heating of an infinite hollow cylinder [8, 9] for the case of a regular regime.

An example of recording the basic parameters (cathode temperature  $T$ , derivative of temperature with respect to time  $dT/d\tau$ , current in the arc  $I$ , and voltage across the arc  $U$ ) in the experiment is shown in Fig. 2. It is seen that the current in the arc discharge and the voltage across it and also the heat flux to the cathode-calorimeter reached their constant values within the first 0.15–0.2 sec. In the same period, the derivative  $dT/d\tau$  also reached an approximately constant value. After about 0.55 sec, the derivative  $dT/d\tau$  de-

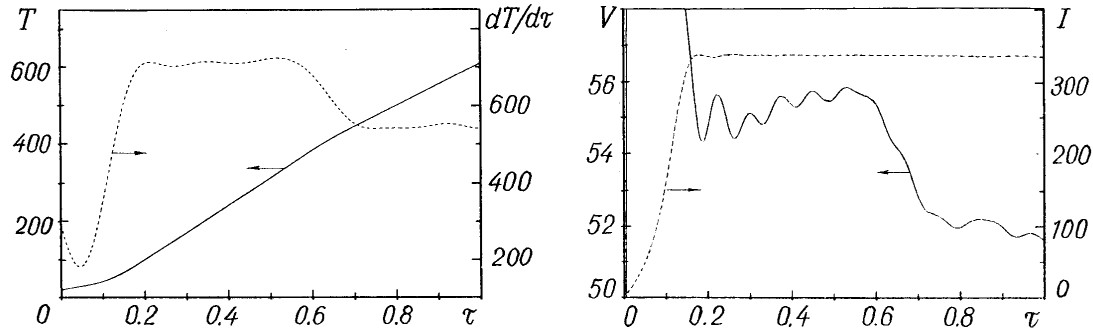


Fig. 2. Records of the heating of a copper cathode (a) and of the current in the arc and the voltage across it (b).

creased markedly with a simultaneous decrease in the voltage across the arc  $V$ . In this case, the value of the current  $I$  was maintained constant (see Fig. 2).

However, the aim of the experiment was to determine not the mean-integral density  $q$  of the heat flux entering the cathode body in accordance with expression (3), but its local density  $q_0$  and the local current density  $j$  inside the cathode arc spot. To pass from the mean-integral density  $q$  to the indicated local densities  $q_0$  and  $j$ , we assumed that the decrease in the derivative  $dT/d\tau$  and the decrease in the heat flux, which were detected at certain temperature  $T_{cr}$  of the ring-cathode surface, are due not to the total fusion of the ring under the action of the heat flux  $q$ , but to the fusion just inside the arc spot, which begins at this moment under the action of the heat flux  $q_0$  having a much higher density. This is substantiated by the fact that the measured value itself of the average surface temperature is much lower than the fusion temperature of copper even in the regime where the derivative  $dT/d\tau$  decreases (see Fig. 2) as well as by the fact that, in our experiments, about 70% of the heat flux entered the cathode through the arc spot. The latter follows from the comparison of the measured heat fluxes with the data of measurements of the thermal volt-equivalent of the arc spot on the copper cathode presented in [4, 5]. Moreover, visual examination of the cathode, performed shortly after the setup had been shut off and the regular regime of heating of the ring had changed to the subsequent regime nonlinear in time  $T = f(\tau)$ , did not reveal marked indications of the total fusion on its surface, and only local fused ring routes were seen.

As has been mentioned above, the setup was shut off automatically at the moment a certain preassigned temperature of the cathode was attained. Changing this limiting temperature gradually, we obtained the sought nonlinear portion at the end of the record, which was seen from the change in the derivative  $dT/d\tau$ . The dimensions of the ring electrode were chosen such that the regular regime ( $Fo_\delta = 0.35$ ) corresponding to the starting point of the linear portion of the record occurred much earlier than the fusion of the electrode in the arc spot [7]. Thus, the time of heating of the ring from the temperature corresponding to the condition  $Fo_\delta = 0.35$  to the temperature causing the fusion to appear in the spot was fairly long, which allowed us to obtain a rather long linear portion of heating necessary for reliable determination of the sought initial moment of fusion.

The procedure of determining the current density in the present work is based on the assumption that an arc spot is a moving surface heat source [3] and on the recording of the average temperature of the electrode surface at the initial moment of fusion. The time of heating of the electrode surface in the spot from the initial temperature  $T$  to the fusion temperature  $T_f$  can be expressed in the form of a simple relation (see [3] and the references cited therein):

$$\tau_0 = \frac{\pi}{4a} \left[ \frac{(T_f - T) \lambda}{q_0} \right]^2. \quad (4)$$

In the macroscopic model of erosion of cold electrodes, a dimensionless parameter  $f$  representing the ratio of the maximum time of heating of a fixed point on the surface of the electrode inside the moving arc spot to the time  $\tau_0$  of its heating to the fusion temperature is widely used [10]:

$$f = \frac{\pi^{1.5} \nu \lambda^2 (T_f - T)^2}{8aj^{1.5} U^2 I^{0.5} n}. \quad (5)$$

Relation (5) is written in a general form suitable for both the jump-like ("step") and the continuous motion of the spot. It has been obtained under the assumption that the maximum time of heating of an electrode point in a moving arc spot can be expressed as  $d/\nu$  if the spot moves continuously or as  $L/\nu$  in the case of a jump-like motion (see [10]) on condition that the heat-flux density is distributed uniformly inside the spot  $q_0 = jU$ . In this formula,  $n$  is the dimensionless step  $n = L/d$ , where  $L$  is the absolute length of the spot "step," i.e., the distance between the subsequent two stops. It was assumed that if the time for which a given point on the electrode is under the action of the heat source (arc spot) is equal to the time of heating of the surface to the fusion temperature, fusion must begin at this point. At this moment, as follows from the definition, the condition  $f = 1$  is fulfilled. For a continuous motion,  $n$  in expression (5) is taken to be equal to unity [10]. If we record the critical temperature of the electrode  $T_{cr}$ , the current  $I$ , and the velocity of the arc  $\nu$  at the initial moment of fusion, then taking the other parameters as known and assuming that  $f = 1$ , we can obtain the sought current density  $j$ :

$$j = \frac{\pi}{4} \left[ \frac{\lambda^2 \nu}{naI^{0.5}} \left( \frac{T_f - T_{cr}}{U} \right)^2 \right]^{2/3}. \quad (6)$$

In the calculations of the effective current density, we used the thermophysical characteristics of the electrode material, which correspond to the middle of the temperature interval of electrode heating (i.e., the interval ambient temperature – fusion temperature). For 700 K, we used the thermal-conductivity coefficient  $\lambda = 377$  W/(m·K) and the thermal diffusivity  $a = 10^{-4}$  m<sup>2</sup>/sec. The velocity of movement of the arc spot over the electrode surface was determined using a magnetic transducer that recorded pulsations of the magnetic field of the current in the ring cathode, and then the Fourier transformation was used to separate the characteristic frequency associated with the movement of the arc spot. To calculate  $j$  in accordance with expression (6), we used the value of the volt-equivalent  $U$  calculated as a function of the magnetic field from the empirical formula

$$U = 6.5 + 4.9B, \quad (7)$$

obtained from special calorimetric investigations using a similar procedure (see [5]). The fusion temperature for commercial copper  $T_f$  was taken to be equal to 1356 K.

As follows from formula (6), to find  $j$  it is also necessary to know the value of the step  $n$ , i.e., it is necessary to monitor the character of motion of the spot. We did not have devices for recording the motion of the spot or for measuring the length of the spot step and set  $n = 1$ . This, of course, introduced a significant error into the value of  $j$ , but taking into account the fact that the data available at the moment differ by a factor of five (see Table 1), such an assumption may be thought of as reasonable at this stage, since it allows one to determine at least the order of  $j$ . In this case, the error can be significantly decreased if a maximum uniform motion of the arc is provided. It is known that the ordered jump-like motion of the arc occurs in the medium of pure atomic inert gases on very pure electrode surfaces or, conversely, on electrodes with thick oxide films possessing dielectric properties [11]. In the medium of molecular gases on cathodes covered with thin oxide films, the movement of the spot is fairly close to a continuous movement.

Moreover, it has been established that in the gap between concentric electrodes, the most unstable motion is the motion of the anode spot, which can destabilize the motion of the entire arc (see [12]). Therefore, to increase the uniformity of the arc motion it is desirable to use small interelectrode gaps, since a cathode jet originating from the cathode spot reaches the anode and serves to move the arc column as a whole together with the cathode and anode spots. For this reason and to provide the predominance of the heat flux entering the cathode through the arc spot over the convective-radiant flux from the arc column, we used small interelectrode gaps in the experiment – 3 mm for electrodes 42–50 mm in diameter. A thick oxide layer also could not be formed on the cathode during the time of the experiment (of the order of 1 sec).

**Experimental Results and Discussion.** As has been mentioned above, Fig. 2a shows a characteristic experimental curve of heating of a cylindrical cathode and its derivative with respect to time. It is apparent that beginning approximately from the instant of time  $\tau = 0.2$  sec and to  $\tau = 0.55$  sec, the derivative  $dT/d\tau$  has a practically constant value. On a record of the derivative  $dT/d\tau$ , there are always some variations caused by changes in the temperature of the ring, whose value is dependent on both the physical and the virtual filters used in the LabView program. From approximately the instant of time 0.55 sec the derivative begins to decrease. At the same time, synchronous with the decrease in the derivative  $dT/d\tau$ , a decrease of 3–4 V in the voltage across the arc occurs (see record in Fig. 2b), which can indicate a possible release of a metal vapor possessing a lower ionization potential as compared to the air. To calculate the current density from formula (6), we used the values of the surface temperature, the arc velocity, and the current, which were recorded at the moment the derivative began to decrease.

The results of the above-described nonstationary experiments carried out on the GWIP setup are denoted by points 1 in Fig. 3. This figure also shows their comparison with the results obtained on the IHMT setup using a similar procedure, but for higher currents – from 1100 to 1400 A (points 2), and also using another, stationary procedure that is considered below (points 3–5) [4, 6]. The results of the experiments carried out on the GWIP setup can be adequately generalized relative to the magnetic field by the exponent (see Fig. 3)

$$j = [2.42 - 1.59 \exp(-B/0.17)] \cdot 10^9. \quad (8)$$

The above-mentioned stationary procedure for determining the current density in the spot was used for processing the experimental data on erosion of electrodes [6]. The experiments were carried out on a setup that also had a copper ring cathode that was only 5 mm in width, but, owing to the cooling, it operated under stationary conditions (see [6]). In this case, the time of the experiments was much longer – from 3 to 20 min. In these experiments, the cathode temperature, current intensity, and arc velocity were measured, which made it possible to obtain, in accordance with formula (6), data on the current density in the cathode arc spot and compare them with the results obtained by the nonstationary method. Figure 4 shows the dependence of the specific erosion  $\gamma$  of a copper cathode on the current, which was found using both cathodes having different diameters (50 and 90 mm) and different magnetic fields (0.03 and 0.133 T). An increase in the diameter of the cathode, all other parameters being the same, significantly influences the temperature conditions of the latter, since the same heat flux spreads over the larger surface of the electrode. For the cathode 50 mm in diameter, some experiments were carried out for a magnetic induction of 0.133 T and some for an induction of 0.03 T, and for the cathode 90 mm in diameter, all the points were obtained for an induction of 0.03 T. In Figs. 3, 4, and 5, identical experiments are represented for convenience by identical points.

As is seen from Fig. 4, for the cathode 50 mm in diameter, the specific erosion is maintained at an approximately constant level (within 2–3  $\mu\text{g}/\text{C}$ ) in the range of currents from 100 to 400 A, while for the cathode 90 mm in diameter, the current range in which this regime is realized is larger and it extends to almost 800 A. When the above critical values of the current (400 and 800 A, respectively) are exceeded, the specific erosion sharply increases. If we assume that the reason for the sharp increase in the erosion for the

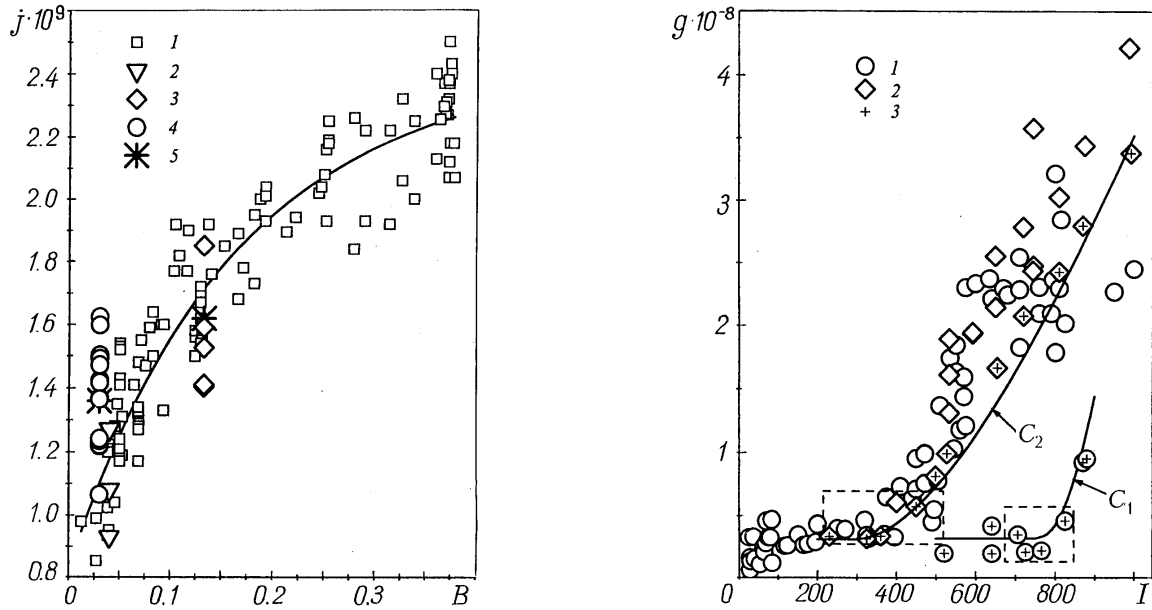


Fig. 3. Results of experiments on determination of the current density in the arc spot on a copper cathode: 1) nonstationary GWIP experiments; 2) nonstationary IHMT experiments for  $B = 0.04$  T [4]; 3) stationary IHMT experiments for  $B = 0.133$  T (see Fig. 4); 4) stationary IHMT experiments for  $B = 0.03$  T; 5) density obtained from the condition of the best approximation of experimental results 3 by theoretical curves  $C_1$  and  $C_2$  (see Fig. 4).

Fig. 4. Dependence of the copper-cathode erosion  $g$  on the current intensity: 1) magnetic induction 0.03 T, the right group of points in the region of curve  $C_1$  corresponds to a cathode diameter of 90 mm, the left group of points in the region of curve  $C_2$  corresponds to a cathode diameter of 50 mm; 3) points obtained in a specially stabilized regime of cooling, air flow rate, and magnetic field on the cathodes 50 mm (points near curve  $C_2$ ) and 90 mm in diameter (points near curve  $C_1$ );  $C_1$  and  $C_2$ , theoretical curves of the best approximation of points 3 by variation of  $j$  using the thermophysical model [3, 4, 6].  $g$ ,  $\text{kg}\cdot\text{C}^{-1}$ .

critical current is the onset of macrofusion of the surface in the arc spot, which corresponds to the condition  $f = 1$ , from relation (6) we can obtain the effective current density in the spot, using the cathode temperature, the arc velocity, and the current, measured under critical conditions.

In Fig. 4, the groups of points found in the dashed frames denote the regions where erosion increases sharply. Having assumed that the condition  $f = 1$  is fulfilled for all these points, we have calculated the current densities in the spot for the used magnetic fields of 0.03 and 0.133 T with the help of expression (6). The results of the measurements and calculations are presented in Table 2 and in Fig. 3 (points 3 and 4). It is seen from Fig. 3 that for a magnetic field of 0.133 T, these "stationary" points 3 obtained on the IHMT setup are distributed approximately uniformly relative to "nonstationary" points 1 obtained on the GWIP setup. For a lower magnetic field of 0.03 T, the results of the stationary experiments (points 4 in the same figure) lie markedly higher than the nonstationary points 1 and the curve approximating them. Points 2 in this figure denote the remaining above-mentioned nonstationary data obtained for a weak magnetic field  $B = 0.04$ , too, and for a current of more than 1 kA on the IHMT setup [4]. Thus, as is seen from Fig. 3, the data



TABLE 2. Current Density  $j$  ( $10^9 \text{ A}\cdot\text{m}^{-2}$ ) in the Cathode Arc Spot Determined by the Stationary Procedure (see points in the dashed frames in Fig. 4)

$I$	$v$	$T$	$j$
$B = 0.03 \text{ T}, U = 6.65 \text{ V}$			
250	54.3	485	1.50
270	54.5	530	1.37
320	58	495	1.42
325	66.5	476	1.60
330	66.4	461	1.62
370	67.4	507	1.47
375	62	585	1.22
395	65.5	472	1.49
440	66	577	1.22
490	63.8	535	1.24
495	55	563	1.07
705	81	472	1.42
725	80	485	1.36
765	87	460	1.47
825	80	518	1.24
$B = 0.13 \text{ T}, U = 7.09 \text{ V}$			
230	91	623	1.59
325	119	573	1.85
360	110	633	1.53
400	111.2	660	1.41
450	128.6	692	1.40

obtained by the nonstationary and stationary methods coincide only for a fairly strong magnetic field (0.133 T), while the data obtained by the nonstationary method coincide for weak magnetic fields (0.03–0.04 T) as well, despite the difference in current (100–400 and 1100–1400 A, respectively). At the same time, for weak magnetic fields the "stationary" data are significantly overestimated as compared to the "nonstationary" data.

In Fig. 4, the groups of points 3 correspond to magnetic fields of 0.03 and 0.133 T. They have been obtained under the same operating conditions of the setup – a constant flow rate of the cooling water and the air and a constant magnetic field as distinguished from the other points obtained for an arbitrary combination of these parameters. Using the thermophysical model of erosion [3, 10] and the method of variation of the current density  $j$ , for these groups of points we have chosen their optimum values that provide the best agreement between the vertical curves  $g(I)$  calculated in accordance with this model and the experiment. The theoretical curves are shown in Fig. 4 as  $C_1$  and  $C_2$  for magnetic fields of 0.03 and 0.133 T, respectively. The obtained optimum values of  $j$  allowed us to represent the dependence of the current density in the spot on the magnetic field in the form of the linear dependence

$$j = (1.282 + 2.6B) \cdot 10^9, \quad (9)$$

whose application to the entire array of experimental data (presented in Fig. 4) obtained with arbitrarily varied parameters made it possible to greatly improve the results of their generalization (see in [6] for details). The current densities obtained using such variation and corresponding to formula (9), are denoted by points 5 in Fig. 3. They coincide approximately with the mean values of  $j$  for points 3 and 4. As is seen from the figure, in the region of magnetic fields  $B = 0.133 \text{ T}$ , relation (9) correlates well with the results of the nonstationary experiments carried out on the GWIP setup (differing from the latter by only 4%), while it gives a

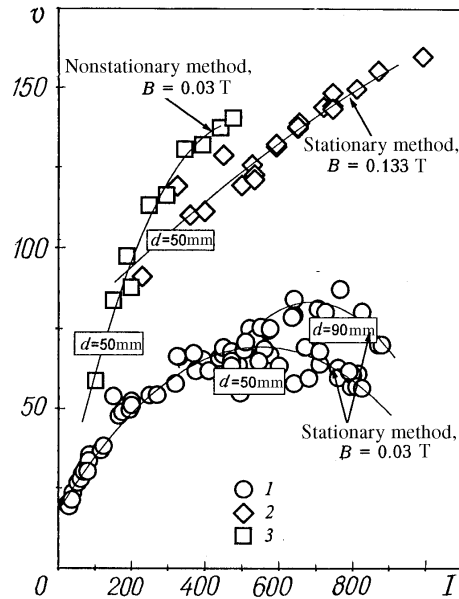


Fig. 5. Arc velocity as a function of the current for constant air flow rates and a constant magnetic field: 1, 2) stationary IHMT experiment (see the notation in Figs. 3 and 4); 3) nonstationary GWIP experiment (see the notation in Fig. 3).

significantly overestimated value of the current density (by almost 30%) as compared to the nonstationary data in the region of lower magnetic fields (0.03 T). As a result, the nonstationary data (points 1 and 2 in Fig. 3) were found to be unsuitable for the stationary experiments on erosion, which are shown in Fig. 4, because of the significant deterioration of the results of the generalization of erosion as compared to those in the case where relation (9) was used (see [6]).

In this connection, we noted the anomalous behavior of the arc velocity in relation to the current in the stationary experiments for the weak magnetic field  $B = 0.03$  T. This anomaly was absent for the stronger magnetic field  $B = 0.133$  T and in the nonstationary experiments. This is illustrated in Fig. 5, in which, as has been mentioned above, identical experiments are denoted by individual points for convenience of comparison with Figs. 3 and 4. Since the arc velocity in a coaxial electric-arc setup is also dependent on the air velocity [13], points obtained for each curve for a constant flow rate of the air are presented here. As is seen from Fig. 5, for the magnetic field  $B = 0.03$  T, when the critical value of the current ( $\approx 500$  A for a cathode 50 mm in diameter and  $\approx 700$  A for a cathode 90 mm in diameter) was exceeded in the stationary experiments, the velocity of motion of the arc decreased and did not increase, as would be expected from the Ampere law for an arc in a magnetic field in accordance with an increase in the driving force  $\vec{F} = \mathbf{I} \times \mathbf{B}$  acting on the arc (see [13]). Points 2 in Fig. 5 indicate that such an anomaly of the arc velocity was absent in the short-duration nonstationary experiments even for a weak magnetic field on the GWIP setup, and for the stronger magnetic field  $B = 0.133$  T it was also absent in the stationary experiments (points 3).

The anomalous behavior of the arc velocity accompanied by a sharp increase in the erosion at the moment of passing through the critical value of the current was also observed by An'shakov et al. [14] under somewhat different conditions – for a tube copper cathode of a vortex electric-arc heater in the region of low magnetic fields – from 0 to 0.02 T. The erosion curves obtained by An'shakov et al. [14] are very similar to our curves  $C_1$  and  $C_2$  in Fig. 4 – they also point to a sharp increase in the erosion for a certain critical current. An'shakov et al. [14] carried out high-speed filming of the motion of the near-electrode region of the arc in the cathode. In this case, they observed the appearance of intense cathode jets originating from the cathode spot for the critical current and a decrease not only in the velocity of arc spot motion, but also in the

rotational velocity of the vortex gas flow as a whole, accompanied by the destruction of the vortex structure under these conditions. An'shakov et al. [14] explained the above-mentioned sharp increase in the cathode erosion by the distortion of the hydrodynamics of the vortex flow for the critical current, which, in their opinion, caused the anomaly of the arc velocity and gave rise to intense cathode jets.

However, our experiments point to the fact that in this case, the initial cause of the velocity anomaly and the sharp increase in the erosion is apparently the microfusion of the spot, which gave rise to the high-power cathode jets detected by the authors, and it is precisely these jets that distorted the hydrodynamics of the vortex flow rather than the reverse. This explains the relation between the erosion and the hydrodynamics of the flow. Thus, when in our experiments the arc was moved by only the magnetic field without the use of a vortex flow, a sharp increase in the erosion for the critical current was observed even in the absence of the velocity anomaly – in the region of stronger magnetic fields equal to 0.133 T. This points to the fact that a sharp increase in the erosion for the critical current was caused by the macrofusion of the spot and not by the velocity anomaly that was observed in our experiments only for weak magnetic fields and was absent for stronger ones.

An indirect proof of the fact that the macrofusion of the spot begins under critical conditions is also a decrease in the voltage across the arc in our nonstationary experiments at the critical cathode temperature, which can indicate the release of a metal vapor from the spot at this temperature. In the nonstationary experiments where thick oxide films were absent on the cathode surface, we did not detect a velocity anomaly, even for the weakest magnetic field  $B = 0.03$  T (points 3 in Fig. 5). The velocity anomaly was observed only in long-duration stationary experiments, i.e., in the case where a fairly thick layer of oxide copper compounds possessing dielectric properties was formed on the cathode surface.

The presence of the velocity anomaly in the case where the arc moves on thick oxide films for weak magnetic fields indicates, in accordance with the data of the high-speed filming in [14], that the continuous motion of the arc changes to an irregular one with periodic stops. Clearly the use of the assumption that  $n = 1$  in formula (6) instead of  $n > 1$  under these conditions led to an overestimation of the obtained values of the current density; this being so, points 4 in Fig. 3 lie higher than the nonstationary data 1 obtained on thin oxide films. This means that, to eliminate the influence of the surface state on the measurement results and obtain more exact data on the current density it is necessary to analyze the character of motion of the spot and measure the length of the spot step.

Thus, the differences in the current densities obtained in the region of weak magnetic fields by stationary and nonstationary thermophysical methods can be explained by the different character of motion of the arc on thick and thin oxide films, which was investigated in [11] and in a number of other works. To further improve the results obtained it is necessary to perform a very complex and laborious diagnostics of the character of motion of the arc spot using special equipment, which can be the subject of another investigation.

**Conclusions.** It has been substantiated experimentally using thermophysical methods that the mean current density in the nonstationary arc spot on a copper cathode increases with increase in the magnetic field, and, for a copper cathode, it can be adequately approximated by an exponential function. Comparison of the results obtained under stationary and nonstationary conditions of heating of the electrode has shown the importance of the diagnostics of the character of motion of the arc spot for further refinement of the data obtained. The new results can be used for calculating the optimum conditions of operation of a copper cathode with minimum erosion, for example, by the procedures proposed in [6].

The authors express their thanks to A. A. do Prado and J. B. Pineiro for technical assistance in the work. We are grateful to scientific foundations of Brazil (CMPq, FAPESP, and FINEP) for financial support of this work.

## NOTATION

$U$ , thermal volt-equivalent, V;  $q$ , heat flux density,  $\text{W}\cdot\text{m}^{-2}$ ;  $Q_0$  and  $q_0$ , heat flux and heat flux density in the arc spot, W and  $\text{W}\cdot\text{m}^{-2}$ , respectively;  $I$  and  $j$ , intensity of the current and its density, A and  $\text{A}\cdot\text{m}^{-2}$ ;  $\lambda$  and  $a$ , coefficients of thermal conductivity and thermal diffusivity of the cathode material,  $\text{W}\cdot\text{m}^{-1}\cdot\text{K}^{-1}$  and  $\text{m}^2\cdot\text{sec}^{-1}$ ;  $\tau$ , time, sec;  $R_1$ ,  $R_2$ , and  $r$ , inner, outer, and running radii of the calorimetric ring, respectively, m;  $K$ , proportionality coefficient;  $T$ , cathode temperature, K;  $T_f$ , fusion temperature of the cathode material, K;  $f$ , dimensionless criterion characterizing the degree of fusion of the electrode surface and the change of the cathode spot from the first to the second type;  $v$ , velocity of motion of the arc spot,  $\text{m}\cdot\text{sec}^{-1}$ ;  $d$ , diameter of the arc spot, m;  $B$ , magnetic induction, T;  $R$ , correlation coefficient; SD, standard deviation. Subscripts: cr, critical value; f, fusion.

## REFERENCES

1. V. I. Rakhovskii, *IEEE Trans. Plasma Sci.*, **PS-4**, No. 2, 81–102 (1976).
2. V. I. Rakhovskii, *Izv. Sib. Otd. Akad. Nauk SSSR, Ser. Tekh. Nauk*, **1**, No. 3, 11–27 (1976).
3. A. Marotta and L. I. Sharakhovskii (Sharakhovsky), *J. Phys. D: Appl. Phys.*, **29**, 2395–2403 (1996).
4. L. I. Sharakhovskii (Sharakhovsky), A. Marotta, and V. N. Borisyyuk, *J. Phys. D: Appl. Phys.*, **30**, 2018–2025 (1997).
5. A. M. Esipchuk, A. Marotta, and L. I. Sharakhovskii, *Inzh.-Fiz. Zh.*, **73**, No. 6, 1245–1254 (2000).
6. L. I. Sharakhovskii (Sharakhovsky), A. Marotta, and V. N. Borisyyuk, *J. Phys. D: Appl. Phys.*, **30**, 2421–2430 (1997).
7. R. H. Kirchhof, *Raketen. Tekh. Kosmon.*, **2**, No. 5, 233–234 (1964).
8. A. V. Luikov, *Theory of Heat Conduction* [in Russian], Moscow (1967).
9. E. P. Trofimov, *Inzh.-Fiz. Zh.*, **3**, No. 10, 47–53 (1960).
10. A. Marotta and L. I. Sharakhovskii (Sharakhovsky), *Heat and Mass Transfer under Plasma Conditions*, Annals of the New York Academy of Sciences, Vol. 891, 36–42 (1999).
11. R. N. Sente, R. J. Munz, and M. G. Drouet, *J. Phys. D: Appl. Phys.*, **23**, 1193–1200 (1990).
12. P. Teste, T. Leblanc, and J.-P. Chabrerie, *J. Phys. D: Appl. Phys.*, **28**, 888–898 (1995).
13. L. I. Sharakhovskii, *Inzh.-Fiz. Zh.*, **20**, No. 2, 306–313 (1971).
14. A. S. An'shakov, A. N. Timoshevskii, and E. K. Urbakh, *Izv. Sib. Otd. Akad. Nauk SSSR, Ser. Tekh. Nauk*, **2**, No. 7, 65–68 (1988).